



King Saud University
Arabian Journal of Chemistry

www.ksu.edu.sa
www.sciencedirect.com



ORIGINAL ARTICLE

Kinetic modeling analysis for the removal of cesium ions from aqueous solutions using polyaniline titanotungstate

I.M. El-Naggar ^a, E.S. Zakaria ^a, I.M. Ali ^a, M. Khalil ^{a,*}, M.F. El-Shahat ^b

^a Atomic Energy Authority, Hot Labs. Center, P. No. 13759, Egypt

^b Faculty of Science, Chemistry Dept., Ain Shams University, Cairo, Egypt

Received 11 July 2010; accepted 27 September 2010

Available online 7 October 2010

KEYWORDS

Sorption;
Kinetics;
Ion exchange;
Polyaniline titanotungstate;
Cesium

Abstract Polyaniline titanotungstate has been synthesized by incorporation of organic polymer polyaniline into the inorganic precipitate of titanotungstate. This material was characterized using X-ray, IR and TGA studies. The influences of initial concentration of metal ions, particle size and temperature have been reported. The comparison of composite and inorganic materials was studied and indicating that the composite material is better than the inorganic in selectivity of Cs⁺ ions. Thermodynamic parameters, such as changes in Gibbs free energy (ΔG), enthalpy (ΔH), and entropy (ΔS) have been calculated. The numerical values of ΔG decrease with an increase in temperature, indicating that the sorption reaction of adsorbent was spontaneous and more favorable at higher temperature. The positive values of ΔH correspond to the endothermic nature of sorption processes and suggested that chemisorptions were the predominant mechanism. A comparison of kinetic models applied to the sorption rate data of Cs⁺ ions was evaluated for the pseudo first-order, the pseudo second-order, intraparticle diffusion and homogeneous particle diffusion kinetic models. The results showed that both the pseudo second-order and the homogeneous particle diffusion models were found to best correlate the experimental rate data. Self diffusion coefficient (D_s), Activation energy (E_a) and entropy (ΔS^*) of activation were also computed from the linearized form of Arrhenius equation.

© 2010 King Saud University. Production and hosting by Elsevier B.V. All rights reserved.

* Corresponding author. Tel.: +20 118649700.
E-mail address: magdykhalil7@yahoo.com (M. Khalil).

1878-5352 © 2010 King Saud University. Production and hosting by Elsevier B.V. All rights reserved.

Peer review under responsibility of King Saud University.
doi:10.1016/j.arabjc.2010.09.028



Production and hosting by Elsevier

1. Introduction

The organic ion exchangers are well known for their uniformity, chemical stability and control of their ion exchange properties through synthetic method (Devi et al., 2010). Inorganic ion exchange materials, besides other advantages, are more stable at high temperatures and in radiation fields than the organic (Amphlett and Jones, 1964; Khan et al., 2009; Alberti et al., 2001; Varshney et al., 2007; Zakaria et al., 2002; El-Naggar et al., 1999; Ali et al., 2008). In order to obtain a combination of these advantages and to increase interlayer

distance of layered inorganic ion exchangers many organic-inorganic exchangers have been developed earlier by the incorporation of organic monomers in the inorganic matrix (Pandit and Chudasama, 1998; Shpeizer et al., 2010; Alberti et al., 2005, 2007; Ferragina et al., 2010). Efforts have been made to improve the chemical, thermal and mechanical stabilities of ion exchangers and to make them highly selective for certain metal ions. Mardan et al. (1999) prepared silica potassium cobalt hexacyanoferrate composite ion exchanger which has excellent exchange properties of ^{137}Cs . Alam et al. (2010) prepared Polyaniline Ce(IV) molybdate that has high selectivity to Cd(II). Inamuddin and Ismail prepared poly-*o*-methoxyaniline Zr(IV) molybdate that has high selectivity to Cd(II) (Inamuddin and Ismail, 2010). Nabi et al. (2009) prepared acrylonitrile stannic(IV) tungstate that has high selectivity to Pb(II). Cobalt ferrocyanide impregnated organic anion exchanger was found to be highly selective for cesium (Valsala et al., 2009). Khan and Inamuddin (2006) prepared Polyaniline Sn(IV) phosphate that was found to be highly selective for Pb(II). polyaniline Sn(IV) tungstoarsenate (Khan et al., 2003) was found to be highly selective for Cd(II). Siddiqui et al. (2007) synthesized a hybrid type of ion exchanger poly(methyl methacrylate) Zr(IV) phosphate that has high selectivity to Pb(II). Polypyrrole thorium(IV) phosphate cation-exchanger was found to be highly selective for pb(II) ion (Khan, 2005).

Polyaniline titanotungstate has been found to have high selectivity for cesium. Cesium removal from aqueous solutions is a major priority of radioactive waste treatment because radio-isotopes of cesium emit gamma radiation, have long half-lives, have a high mobility in the biosphere and have hazardous effect on the environment (Lebedev et al., 2003; Zakaria and El-Naggar, 1998). Cesium is, therefore, a potential pollutant in the environment. The following pages summarized synthesis, characterization and Sorption kinetic modeling analysis for the removal of cesium ions from aqueous solutions using this material.

2. Experimental

2.1. Reagents

All reagents and chemicals utilized in this work were of analytical grade purity. The reagents used for the synthesis of material were obtained from PROLABO, FLUKA and ADWIK. Bidistilled water was used for solutions preparation, dilution and washing all glass.

2.2. Preparation of the reagent solutions

A solution (1 M) of titanium chloride, $\text{TiCl}_4 \cdot \text{H}_2\text{O}$ was prepared in 4 M-HCl, while 1 M sodium tungstate, $\text{Na}_2\text{WO}_2 \cdot 2\text{H}_2\text{O}$ solution was prepared in demineralized water (DMW). Solutions of 10% (v/v) aniline ($\text{C}_6\text{H}_5\text{NH}_2$) and 0.1 M potassium persulphate ($\text{K}_2\text{S}_2\text{O}_8$) were prepared in 1 M HCl.

2.3. Preparation of polyaniline titanotungstate

Polyaniline gels were prepared by mixing aqua volumes of the solutions of 10% aniline ($\text{C}_6\text{H}_5\text{NH}_2$) and 0.1 M potassium persulphate with continuous stirring by a magnetic stirrer. Green colored polyaniline gels were obtained by keeping the solutions below 10 °C for half an hour. A precipitate of titanium tung-

state was prepared at $(65 \pm 2^\circ\text{C})$ by adding 1 M titanium chloride solution to an aqueous solution of 1 M sodium tungstate ($\text{Na}_2\text{WO}_2 \cdot 2\text{H}_2\text{O}$) in equal volume ratio. The white precipitates were obtained, when the pH of the mixtures was adjusted to 6.5 by adding aqueous ammonia with constant stirring. The gels of polyaniline were added to the white inorganic precipitate of titanium and mixed thoroughly with constant stirring. The resultant green colored gels were kept for 24 h at room temperature $(25 \pm 2^\circ\text{C})$ for digestion. The supernatant liquid was decanted and the gel was rewashed with bidistilled water in order to remove fine adherent particles and was filtered by center fission. The excess acid was removed by washing with DMW and the material was dried in an air oven at 50 °C. The dried products were immersed in DMW to obtain small granules. They were converted into H-form by treating with 0.01 M HNO_3 for 24 h with occasional shaking intermittently replacing the supernatant liquid with fresh acid. The excess acid was removed after several washings with DMW and then dried at 50 °C. Materials of several particles size were obtained by sieving and kept in desiccators.

2.4. Instruments and characterization of polyaniline titanotungstate

Measurements of powder X-ray diffraction patterns were carried out using Shimadzu X-ray diffractometer, Model XD 490 Shimadzu, Kyoto, Japan, with a nickel filter and Cu-K_α radiation tube. Samples were very lightly ground and mounted on a flat sample plate at room temperature. Measurements of differential thermal analysis (DTA) and thermogravimetric analysis (TG) were carried out using a Shimadzu DTA-60 thermal analyzer obtained from Shimadzu Kyoto, Japan. The sample was measured from ambient temperature up to 1000 °C with the heating rate of 20 °C/min. The IR spectrum of the prepared materials was measured by IR spectrometer using KBr disc technique. The IR spectrum was scanned over the wave length range 400–4000 cm^{-1} using BOMEM FTIR model MB 147, product from Canada. An elemental analyzer caring using a double beam atomic absorption spectrophotometer was obtained from Shimadzu, Kyoto, Japan, and an inductively coupled plasma mass spectrophotometer (ICP) was obtained from Shimadzu, Kyoto, Japan.

2.5. Kinetic studies

Kinetic measurements were performed, using batch technique, by equilibrating 0.05 g of each of polyaniline titanotungstate (composite) and inorganic compound titanotungstate (inorganic) with $V/m = 50 \text{ cm}^3/\text{g}$ with three different concentrations of 660, 1300 and 6600 mg/L of Cs^+ ions. The experiments were also conducted at three different reaction temperatures $(25, 45 \text{ and } 60 \pm 1^\circ\text{C})$, and three different particle diameters 0.46, 0.318 and 0.156 mm using an initial ion concentration of 1300 mg/L. For these investigations 0.05 g of polyaniline titanotungstate and the inorganic compound titanotungstate was contacted with 2.5 ml of solution containing known concentration of Cs^+ ($V/m = 50 \text{ cm}^3/\text{g}$) and the solution was kept stirred in a thermostatic shaker adjusted at the desired temperature as a function of the time. After interval time, the shaker is stopped and the solution is separated at once from the solid. The solution was analyzed using atomic absorption in order to determine the amount of Cs^+ ions sorbet. The amount of metal ion sorbet

onto polyaniline titanotungstate and inorganic compound titanotungstate at any time, q_t (mg/g) and the sorption (P) were calculated from the expressions:

$$q_t = (c_0 - c_t) \frac{V}{m} \quad (1)$$

$$P = \left(\frac{C_0 - C_t}{C_0} \right) \times 100 \quad (2)$$

where C_0 is the initial concentration, C_t is the concentration at time t (mg/L) of metal ions in solution, V the volume (L) and m is the weight (g) of the adsorbent.

3. Results and discussion

3.1. Characterization of polyaniline titanotungstate

Fig. 1 shows the FTIR spectrum of polyaniline (a), titanotungstate (b), and polyaniline titanotungstate (c). It is evident from

the FTIR studies of the 'organic-inorganic' composite cation-exchanger in H^+ -form polyaniline titanotungstate (Fig. 1c) that the material shows the presence of external water molecule in addition to $-OH$ groups and the metal oxygen bond. In the spectrum of the material, a strong and broad band around 3287 cm^{-1} is found which can be ascribed to $-OH$ stretching frequency. A sharp peak around 1615 cm^{-1} can be attributed to $H-O-H$ bending band, representing the free water molecules (water of crystallization) which represents the strongly bonded $-OH$ groups in the matrix (Rao, 1993). The band appearing at 1400 cm^{-1} may correspond to the Ti and $W-OH$ bonds (Rawat et al., 1990; Nabi and Shalla, 2009). In the polyaniline (Fig. 1a) the peaks at about 1476 cm^{-1} due to the $N-H$ bending vibration, the $C-N$ stretching vibration in the region 1299 cm^{-1} , the $N-H$ rocking at 796 cm^{-1} and $C=C$ at 1562 cm^{-1} indicate the presence of polyaniline. In the polyaniline titanotungstate (Fig. 1c), there is $C-N$ stretching band around 1299 cm^{-1}

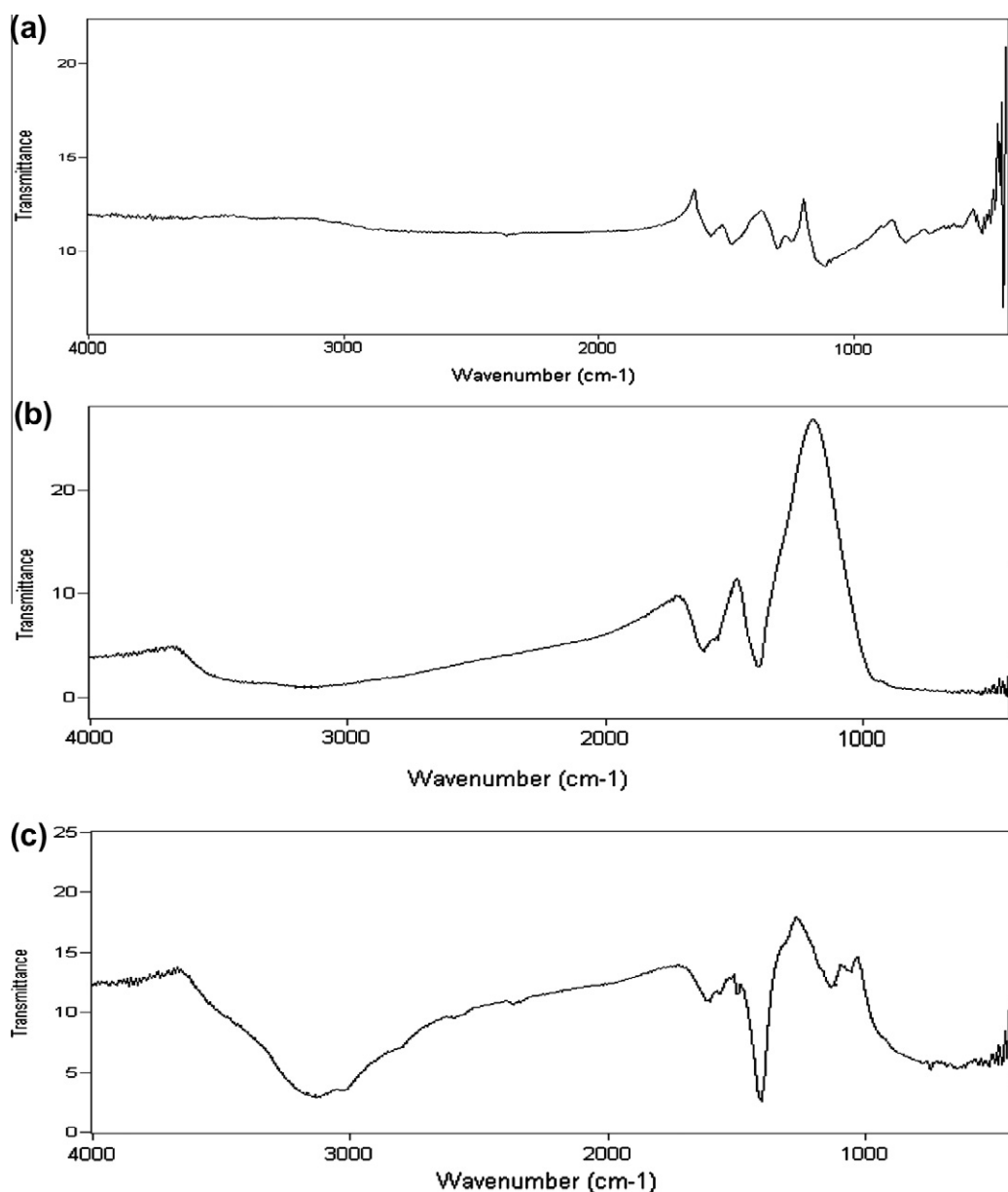


Figure 1 FTIR spectra of a prepared polyaniline (a), titanotungstate (b), and polyaniline titanotungstate composite material (c).

region and C–C stretching band around 1139 cm^{-1} . These characteristic stretching frequencies show close resemblance with the inorganic precipitate, i.e. in polyaniline titanotungstate (Fig. 1c), indicating the binding of inorganic precipitate with organic polymer and formation of ‘organic–inorganic’ composite ‘polyaniline titanotungstate.’ This indicates that the polyaniline titanotungstate contains considerable amount of aniline.

The X-ray diffraction pattern of the synthesized polyaniline titanotungstate is amorphous. The TGA–DTA analysis curve (Fig. 2) of the polyaniline titanotungstate showed a continuous loss of mass (about 10%) up to $130\text{ }^{\circ}\text{C}$, which may be due to the removal of the water of crystallization (Ali et al., 2010). A further mass loss between 230 and $730\text{ }^{\circ}\text{C}$ may be due to complete decomposition of the organic part of the material. Above $730\text{ }^{\circ}\text{C}$, a smooth horizontal section is seen, which rep-

resents the complete formation of the oxide form of the material. The total loss of weight is 17% up to $1000\text{ }^{\circ}\text{C}$ indicating that the material is stable.

3.2. Effect of initial concentration and contact time

The effect of the initial ion concentration was performed at initial concentrations of 660, 1300 and 6600 mg/L at $25\text{ }^{\circ}\text{C}$ for the sorption of Cs^+ ions onto polyaniline titanotungstate and inorganic compound titanotungstate and the results were shown in Fig. 3. It is clear that the sorption amount of Cs^+ ions increase with increasing the initial ion concentration, and the amount of Cs^+ ions sorbet by composite is grater than that of Cs^+ ions sorbet by inorganic adsorbent. Also, the amount of Cs^+ ions sorbet sharply increases for each adsorbent with time in the initial stage (0–120 min range), and then

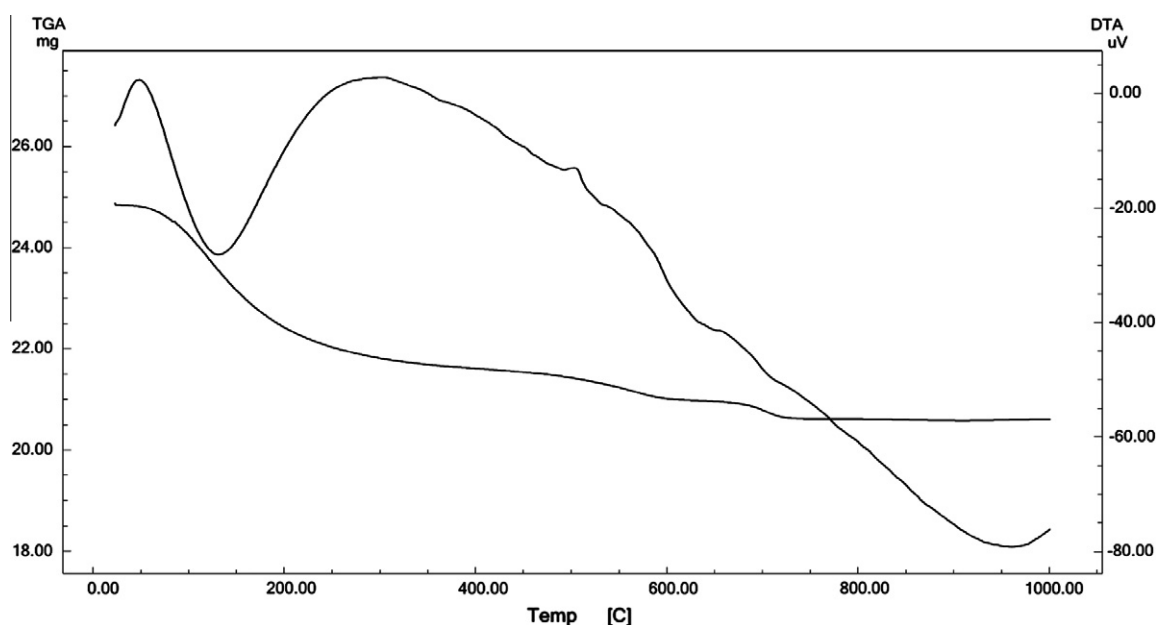


Figure 2 TGA–DTA thermogram of polyaniline titanotungstate.

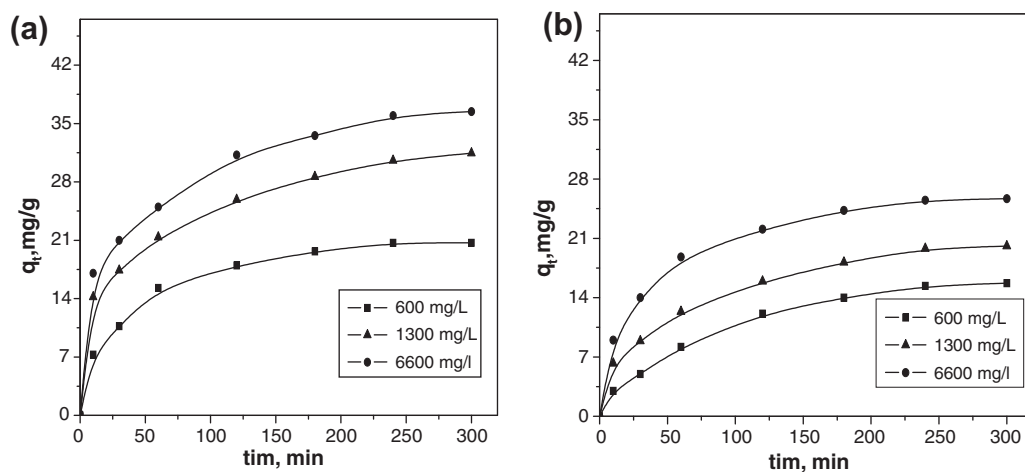


Figure 3 Effect of initial ion concentration and contact time on the amount sorbet of Cs^+ ions onto (a) polyaniline titanotungstate and (b) titanotungstate.

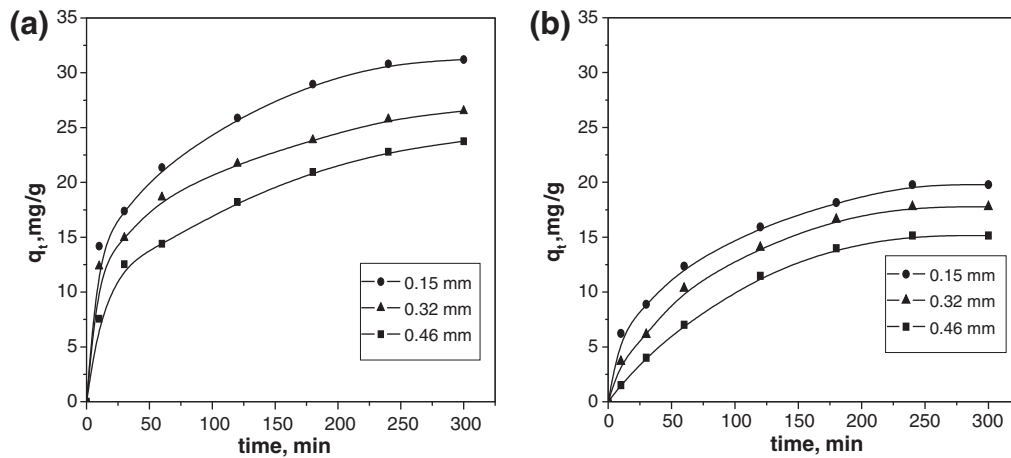


Figure 4 Plots of the amount sorbed of Cs^+ ions onto (a) polyaniline titanotungstate and (b) titanotungstate at different particle sizes.

gradually increases to reach an equilibrium value in approximately 240 min. A further increase in contact time had a negligible effect on the amount of ion sorption. The rate of reaction was found to be independent of the initial concentration. According to these results, the agitation time was fixed at 5 h for the rest of the batch experiments to make sure that the equilibrium was reached. The increase in the uptake capacity of the adsorbent material with increasing initial ion concentration may be due to higher probability of collision between each investigated ion and the adsorbent particles. The variation in the extent of sorption may also be due to the fact that initially all sites on the surface of adsorbent were vacant and the metal ion concentration gradient was relatively high. Consequently, the extent of each ion uptake decreases significantly with the increase of contact time, depending on the decrease in the number of vacant sites on the surface of adsorbent material.

3.3. Effect of particle size

Fig. 4 shows plots of the amount sorbed of Cs^+ ions from aqueous solutions for various adsorbent particle sizes. The adsorbent diameters shown are the averages of the mesh sizes

for the consecutive sieves that allowed the particles to pass through and retained the particles. It is clear from the figure that the metal ion removal rate was significantly affected by the particle size. The rate and extent of sorption, for a constant mass of the adsorbent, is proportional to the specific surface area, which is higher for small particles. Guibal et al. (1998) reported that mathematical models for external surface diffusion and intraparticle diffusion controlled sorption dictated that the sorption rate parameters should vary with the reciprocal of the first power of the adsorbent particle diameter and the reciprocal of some power of the adsorbent particle diameter, respectively. On the other hand, if the interaction between the sorbed and the binding sites is kinetically rate controlled, the rate constant, and hence sorption rate will be independent of the adsorbent particle size (Ho and McKay, 1999a).

3.4. Effect of contact time and temperature

Fig. 5 shows plots of the amount sorbed of Cs^+ ions from aqueous solutions onto prepared polyaniline titanotungstate and titanotungstate, at initial metal ion concentration 1300 mg/L and at temperature 25, 45 and 60 °C as a function of contact

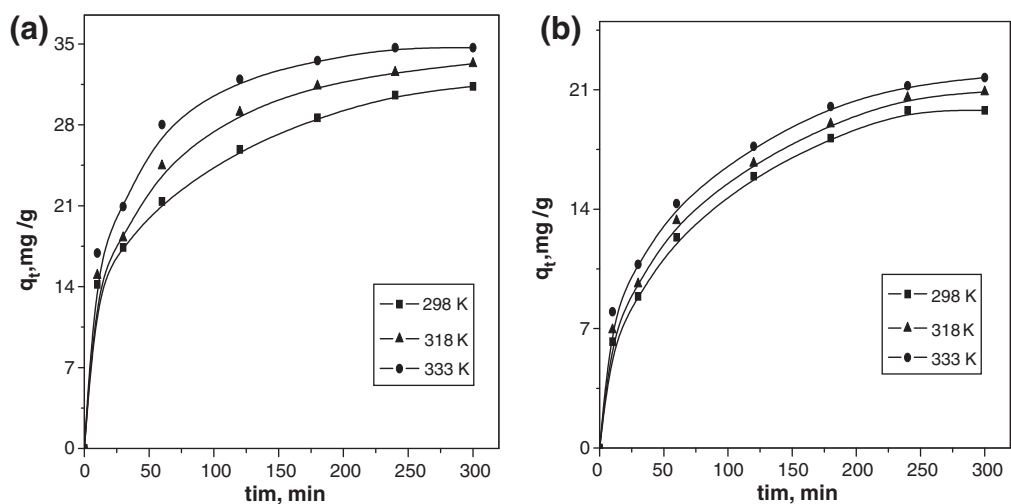


Figure 5 Effect of contact time on the amount sorbed of Cs^+ ions onto (a) polyaniline titanotungstate and (b) titanotungstate at different temperatures.

time. The figure shows a high initial rate of removal within the first 120 min of contact (over 80% removed) followed by a slower subsequent removal rate that gradually approached an equilibrium conditions in 5 h. The thermodynamics parameters for the systems were calculated at different temperatures and summarized in Table 1. In order to gain insight into the thermodynamic nature of the sorption process, several thermodynamic parameters for the present systems were calculated. The Gibbs free energy change, ΔG , is the fundamental criterion of spontaneity. Reactions occur spontaneously at a given temperature if ΔG is a negative quantity. The free energy of the sorption reaction is given by the following equation:

$$\Delta G = -RT \ln K_c$$

where K_c is the sorption equilibrium constant, R the gas constant, and T is the absolute temperature (K). The sorption equilibrium constant (K_c) can be calculated from:

$$K_c = \frac{F_e}{1 - F_e} \quad (4)$$

where F_e is the fraction attainment of metal ion sorbet at equilibrium.

The values of the equilibrium constant (K_c) for the sorption of Cs^+ ions onto composite and inorganic adsorbent were calculated at different temperatures and at equilibrium time of 5 h using Eq. (4). The variation of K_c with temperature, as summarized in Table 1, showed that K_c values increase with increase in sorption temperature, thus implying a strengthening of adsorbate-adsorbent interactions at higher temperature. This also indicates that Cs^+ ions dehydrate considerably at higher temperature before sorption and thus their sizes during sorption are smaller yielding higher K_c values (Ho and McKay, 1999b). Also, the obtained negative values of ΔG confirm the feasibility of the process and the spontaneous nature of the sorption processes with preference towards Cs^+ ions.

The Gibbs free change can be represented as follows:

$$\Delta G = \Delta H - T\Delta S \quad (5)$$

The values of enthalpy change (ΔH) and entropy change (ΔS) calculated from the slope and intercept of the plot of ΔG versus T (Fig. 6) are also given in Table 1. The value of ΔH for Cs^+ ions was found to be positive, the reaction is endothermic. The positive values of the entropy change (ΔS) show the increased randomness at the solid/solution interface with some structural changes in the adsorbate and adsorbent and an affinity of the polyaniline titanotungstate and titanotungstate towards Cs^+ ions.

3.5. Sorption kinetics modeling

The study of sorption dynamics describes the solute uptake rate and evidently this rate controls the residence time of

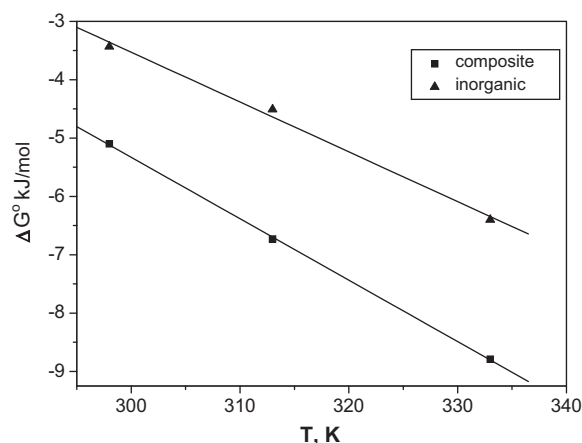


Figure 6 Relationship between Gibbs free energy change and temperature of sorption of Cs^+ ions onto polyaniline titanotungstate and titanotungstate at different temperatures.

adsorbate uptake at the solid/solution interface. In this part of study, the data of the kinetics of Cs^+ ions sorbet from aqueous solutions onto prepared polyaniline titanotungstate and titanotungstate at different temperatures, as illustrated in Fig. 5, were analyzed using pseudo first-order, pseudo second-order, intraparticle diffusion and homogeneous particle diffusion kinetic models, respectively. The conformity between experimental data and each model predicted values was expressed by the correlation coefficient (R^2). A relatively high R^2 values indicates that the model successfully describes the kinetics of metal ion sorption removal.

3.5.1. Pseudo first-order model

The sorption kinetics of metal ions from liquid phase to solid is considered as a reversible reaction with an equilibrium state being established between two phases. A simple pseudo first order model (Ho and McKay, 1999a,b) was, therefore, used to correlate the rate of reaction and expressed as follows:

$$\frac{dq_t}{dt} = k_1(q_e - q_t) \quad (6)$$

where q_e and q_t are the concentrations of ion in the adsorbent at equilibrium and at time t , respectively, (mg/g) and k_1 is the pseudo first-order rate constant (h^{-1}).

After integration and applying boundary conditions $t = 0$ to $t = t$ and $q_t = 0$ to $q_t = q_t$, the integrated form of Eq. (6) becomes:

$$\log(q_e - q_t) = \log q_e - \frac{k_1}{2.303}t \quad (7)$$

Plots for Eq. (7) were made for Cs^+ ions sorption at different studied temperatures and shown in Fig. 7. Approximately

Table 1 Equilibrium characteristics and thermodynamic parameters for the sorption of Cs^+ ions on polyaniline titanotungstate and (b) titanotungstate at different temperatures.

Temperatures (K)	K_c		ΔG (KJ/mol)		ΔH (KJ/mol)		ΔS (J/mol K)	
	Com.	Inorg.	Com.	Inorg.	Com.	Inorg.	Com.	Inorg.
298	7.84	4.00	-5.103	-3.43	26.26	22.08	105.3	85.38
318	13.2	5.66	-6.73	-4.51				
333	24.00	10.11	-8.79	-6.40				

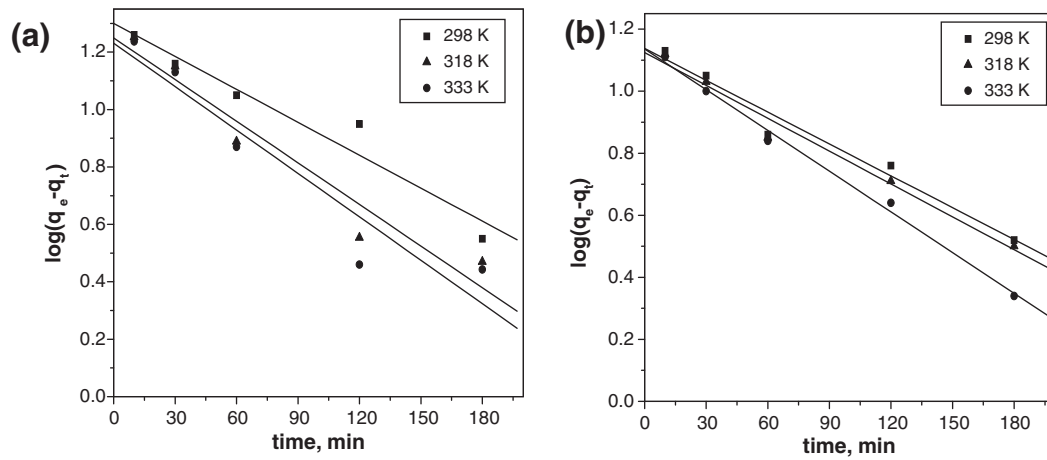


Figure 7 Pseudo first-order kinetic plots for the sorption of Cs^+ ions from aqueous solutions onto (a) polyaniline titanotungstate and (b) titanotungstate at different temperatures.

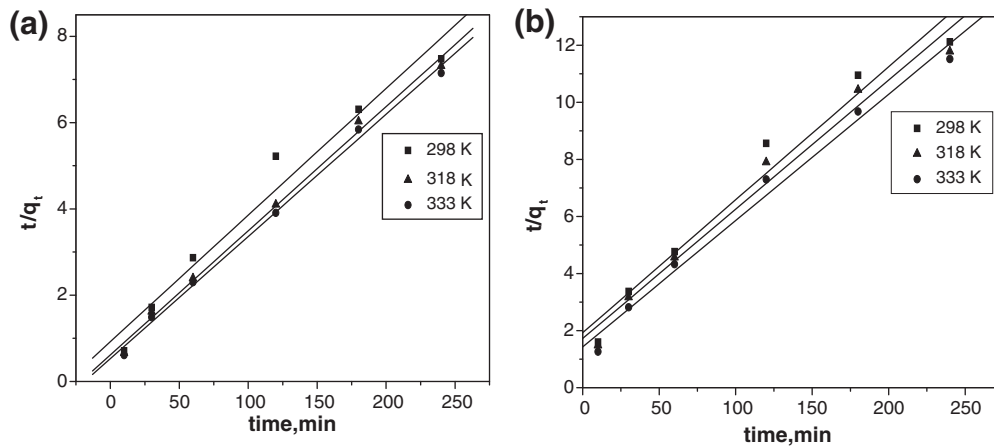


Figure 8 Pseudo second-order kinetic plots for the sorption of Cs^+ ions from aqueous solutions onto (a) polyaniline titanotungstate and (b) titanotungstate at different temperatures.

linear fits were observed for the two adsorbent, over the entire range of shaking time explored and at all temperatures, with low correlation coefficients, indicating that the pseudo first-order kinetic model is not valid for the present systems.

3.5.2. Pseudo second-order model

A pseudo second-order rate model (Ho and McKay, 1999b,c) is also used to describe the kinetics of the sorption of ions onto adsorbent materials. The differential equation for chemisorptions kinetic rate reaction is expressed as:

$$\frac{dq_t}{dt} = k_2(q_e - q_t)^2 \quad (8)$$

where k_2 is the rate constant of pseudo second-order equation (L/mg h).

For the boundary conditions $t = 0$ to $t = t$ and $q_t = 0$ to $q_t = q_t$, the integrated form of Eq. (8) becomes:

$$\frac{1}{q_e - q_t} = \frac{1}{q_e} + k_2 t \quad (9)$$

Table 2 The calculated parameters of the pseudo second-order kinetic models for Cs^+ ions onto (a) polyaniline titanotungstate and (b) titanotungstate at different temperatures.

Temperature (K)	q_e (mg/g) experimental		q_e (mg/g) calculated		h (mg/L h)		K_2 (L/mg h)		R^2	
	Com.	Ino.	Com.	Ino.	Com.	Ino.	Com.	Ino.	Com.	Ino.
278	32.08	19.79	34.083	21.46	64.8	31.2	1.91	1.45	0.9840	0.9829
318	32.79	20.36	34.75	22.10	97.2	34.8	2.76	1.56	0.9973	0.988
333	33.5	20.82	35.32	22.58	112.8	41.4	3.18	1.8	0.9979	0.9930

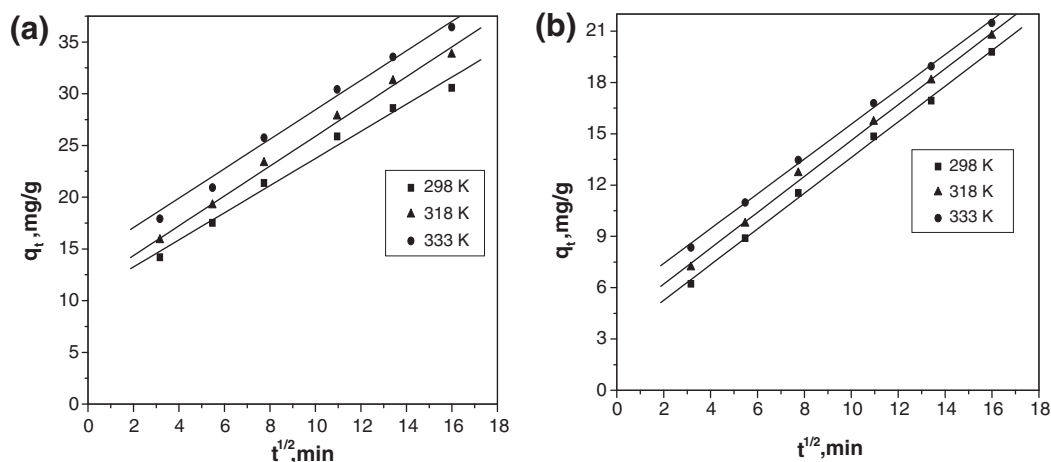


Figure 9 Morris–Weber kinetic plots for the sorption of Cs^+ ions from aqueous solutions onto (a) polyaniline titanotungstate and (b) titanotungstate at different temperatures.

Eq. (9) can be rearranged to obtain a linear form equation as:

$$\left(\frac{t}{q_t}\right) = \left(\frac{1}{k_2 q_e^2}\right) + \left(\frac{1}{q_e}\right)t \quad (10)$$

If the initial sorption rate h (mg/L h) is:

$$h = k_2 q_e^2 \quad (11)$$

Then Eqs. (10) and (11) become:

$$\frac{t}{q_t} = \frac{1}{h} + \frac{1}{q_e} t \quad (12)$$

The kinetic plots of t/q_t versus t for Cs^+ ions sorption at different temperatures are presented in Fig. 8. The relationships are linear, and the values of the correlation coefficient (R^2), suggest a strong relationship between the parameters and also explain that the process of sorption of each ion follows pseudo second order kinetic model. From Table 2, it can be shown that the values of the initial sorption rate ' h ' and rate constant ' k_2 ' were increased with increase in temperature. The correlation coefficient R^2 has an extremely high value (>0.98), and the theoretical q_e values agree with the experimental ones. These results suggest that the pseudo second-order sorption mechanism is predominant and that the over all rate constant of each sorbent appears to be controlled by the chemisorptions process.

3.5.3. Intraparticle diffusion model

The intraparticle diffusion model, Morris and Weber model (Weber and Morris, 1963), is expressed as:

$$q_t = k_{\text{ad}} t^{1/2} + c \quad (13)$$

where K_{ad} is the rate constant of intraparticle transport ($\text{mg/g min}^{1/2}$), and c is the boundary layer diffusion. According to this model, plotting a graphic of q_t versus $t^{1/2}$, if a straight line with intercept c is obtained, it can be assumed that the involved mechanism is a diffusion of the species as shown in Fig. 9. In this case the slope of the linear plot is the rate constant of intraparticle transport. The values of K_{ad} were calculated, from the slope of the linear plots obtained, and the values of C were calculated from the intercept that presented in Table 3.

3.5.4. Homogeneous particle diffusion model (HPDM)

In this model, the rate-determining step of sorption is normally described by either (a) diffusion of ions through the liquid film surrounding the particle, called film diffusion, or (b) diffusion of ions into the sorbent beads, called particle diffusion mechanism. Nernst–Plank equation (Helfferich, 1962), which takes into account both concentration and electrical gradients of exchanging ions into the flux equation, was used to establish the HPDM equations. If the diffusion of ions from the solution to the sorbent beads is the slowest step, rate-determining step, the liquid film diffusion model controls the rate of sorption. In such case, the following relation can be utilized to calculate the diffusion coefficient:

$$-\ln(1 - F) = \frac{3D_i C}{r_0 \delta C_r} t \quad (14)$$

where C and C_r are the equilibrium concentrations of the ion in solution and solid phases, respectively, D_i the diffusion coefficient in the liquid phase, F the fraction attainment of equilibrium or extent of adsorbent conversion, r_0 the radius of the adsorbent particle, and δ is the thickness of the liquid film.

Table 3 Intraparticle diffusion rate constant for the sorption Cs^+ ions onto polyaniline titanotungstate and titanotungstate at different temperatures.

Temperature (K)	k_{ad} ($\text{mg/g min}^{1/2}$)		Intercept (C)		R^2	
	Com.	Inorg.	Com.	Inorg.	Com.	Inorg.
298	1.311	1.043	10.627	3.172	0.9933	0.999
318	1.441	1.049	11.473	4.109	0.97413	0.9987
333	1.46	1.072	14.212	5.38	0.957	0.999

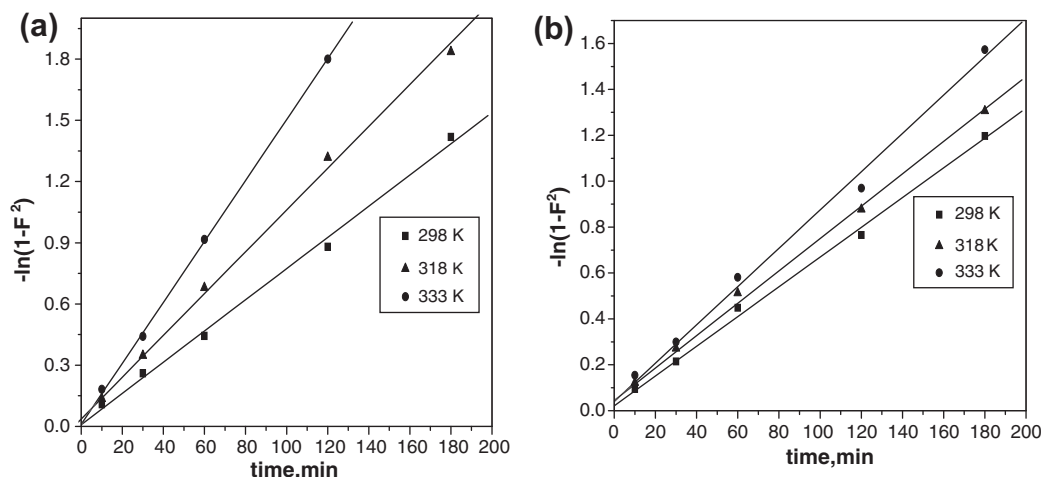


Figure 10 Plots of $-\ln(1-F^2)$ as a function of time for the diffusion of Cs^+ ions onto (a) polyaniline titanotungstate and (b) titanotungstate at different temperatures.

If the diffusion of ions through the adsorbent beads is the slowest step, the particle diffusion will be the rate-determining step and the particle diffusion model could apply to calculate the diffusion coefficients. Then, the rate equation is expressed by:

$$-\ln(1-F^2) = \frac{3D_i\pi^2}{r_0^2}t \quad (15)$$

where D_i is the particle diffusion coefficient.

The two previous model equations (Eqs. (14) and (15)) were tested against the kinetic rate data of both polyaniline titanotungstate and titanotungstate at different temperatures for Cs^+ ions by plotting the functions of $-\ln(1-F)$ and $-\ln(1-F^2)$ against contact time. The straight lines that are obtained in the case of $-\ln(1-F)$ versus time do not pass through the origin (graphs omitted), indicating that the film diffusion model does not control the rate of the sorption processes. On the other hand, the straight lines of the plots of $-\ln(1-F^2)$ versus contact time, as shown in Fig. 10, pass through the origin for both ions indicating that the particle diffusion model controls the sorption processes at all studied temperatures. The slope values of these plots were used to calculate the effective diffusion coefficients (D_i) using Eq. (15). These calculated values together with the correlation coefficient (R^2) for both exchangers are presented in Table 4.

The magnitude of the diffusion coefficient is dependent upon the nature of the sorption process. For physical adsorption, the value of the effective diffusion coefficient ranges from 10^{-6} to 10^{-9} m^2/s and for chemisorptions, the value ranges from 10^{-9} to 10^{-17} m^2/s (Walker and Weatherley,

1999). The difference in the values is due to the fact that in physical adsorption the molecules are weakly bound and, therefore, there is ease of migration, whereas for chemisorptions the molecules are strongly bound and mostly localized. Therefore, from this research, the most likely nature of sorption is chemisorptions since the values of D_i were in the order 10^{-12} m^2/s for both exchangers. This is in agreement with the pseudo second-order kinetic model. Also, based on the values of the correlation coefficient (R^2) obtained for all tested models, the pseudo second-order and PHDM models were found to best correlate the rate kinetic data of the sorption of Cs^+ ions.

On the other hand, plotting of $\ln D_i$ versus $1/T$ gave a straight line, as shown in Fig. 11, proves the validation of the linear form of Arrhenius equation:

$$\ln D_i = \ln D_o - \left(\frac{E_a}{RT}\right) \quad (16)$$

where D_o is a pre-exponential constant analogous to Arrhenius frequency factor.

The energies of activation of Cs^+ ions for both adsorbent, E_a , were calculated from the slope of the straight lines in Fig. 11 and the obtained values were presented in Table 5.

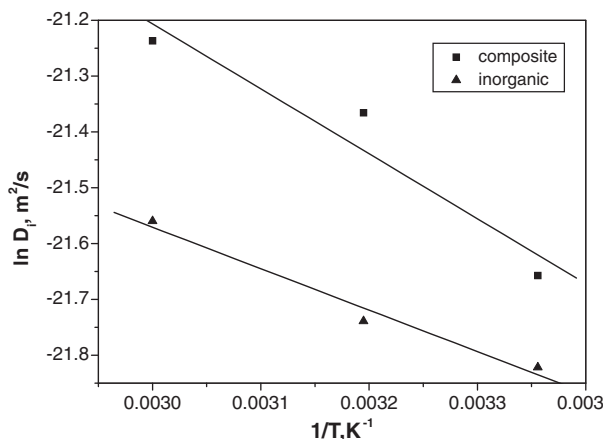


Figure 11 Arrhenius plots for the particle diffusion coefficients of Cs^+ ions sorbet onto polyaniline titanotungstate and titanotungstate.

Table 4 Diffusion coefficients for the sorption of Cs^+ ions onto polyaniline titanotungstate and titanotungstate.

Temperature (K)	$D_i \times 10^{-12}$ (m^2/s)		R^2	
	Com.	Ino.	Com.	Ino.
298	3.93	3.33	0.998	0.998
313	5.26	3.62	0.998	0.998
333	5.98	4.29	0.999	0.997

Table 5 Kinetic parameters for the sorption of Cs⁺ ions onto polyaniline titanotungstate and titanotungstate.

Adsorbent	D_0 (m ² /s)	Ea (kJ/mol)	ΔS^* (J/mol K)
Composite	0.202×10^{-9}	9.66	-120.96
Inorganic	3.98×10^{-9}	6.17	-134.53

Values of Ea below 42 kJ/mol generally indicate diffusion-control processes and higher values represent chemical reaction processes (Scheckel and Sparks, 2001). Such a low value of the activation energy for the sorption of each adsorbent indicates a chemical sorption process involving weak interaction between adsorbents, and sorbet Cs⁺ and suggests that each sorption process has a low potential energy. The Arrhenius equation would be also used to calculate D_0 , which in turn is used for the calculation of entropy of activation (ΔS^*) of the sorption process using (Mohan and Singh, 2002):

$$D_0 = \left(\frac{2.72d^2KT}{h} \right) \exp \left(\frac{\Delta S^*}{R} \right) \quad (17)$$

where K is the Boltzmann constant, h the Plank constant, d the distance between two adjacent active sites in the solid matrix, R the gas constant, and T is the absolute temperature. Assuming that the value of d is equal to 5×10^{-8} cm (Mohan and Singh, 2002), the values of ΔS^* for both adsorbents were calculated and presented in Table 5. The value of entropy of activation (ΔS^*) is an indication of whether or not the reaction is an associative or dissociative mechanism. ΔS^* values > -10 J/mol K generally imply a dissociative mechanism (Scheckel and Sparks, 2001). However, the high negative values of ΔS^* obtained in this study (Table 5) suggested that Cs⁺ ions sorption on each of polyaniline titanotungstate and titanotungstate is an associative mechanism.

4. Conclusion

Polyaniline titanotungstate and titanotungstate were chemically prepared, characterized using DTA-TGA, XRD, IR and tested as adsorbent material for the removal of cesium ions from aqueous solutions. Polyaniline titanotungstate was more selective for Cs⁺ ions than titanotungstate. The kinetics of both adsorbents were experimentally studied and the obtained rate data were analyzed using the pseudo first-order, the pseudo second-order, intraparticle diffusion and homogeneous particle diffusion kinetic models. Based on the values of the correlation coefficient (R^2) obtained for all tested models, both pseudo second-order and PHDM models were found to best correlate the rate kinetic data of both adsorbent. The magnitudes of the particle diffusion coefficients of both adsorbents were in the order of 10^{-12} m²/s indicating a chemisorption nature for the sorption processes. The values of Ea obtained are < 42 kJ/mol, indicating a diffusion-controlled process and based on ΔS^* values, the sorption reaction of each adsorbent are an associative mechanism.

References

Alam, Z., Inamuddin, Nabi, S.A., 2010. Synthesis and characterization of a thermally stable strongly acidic Cd(II) ion selective composite

cation-exchanger: polyaniline Ce(IV) molybdate. *Desalination* 250 (2), 515–522.

- Alberti, G., Cavalaglio, S., Marmottini, F., Matusek, K., Megyeri, J., Szirtes, L., 2001. Preparation of a composite γ -zirconium phosphate-silica with large specific surface and its first characterisation as acid catalyst. *Applied Catalysis* 218 (1–2), 219–228.
- Alberti, G., Casciola, M., Donnadio, A., Piaggio, P., Pica, M., Sisani, M., 2005. Preparation and characterisation of α -layered zirconium phosphate sulfophenylphosphonates with variable concentration of sulfonic groups. *Solid State Ionics* 176 (39–40), 2893–2898.
- Alberti, G., Casciola, M., Capitani, D., Donnadio, A., Narducci, R., Pica, M., Sganappa, M., 2007. Novel Nafion–zirconium phosphate nanocomposite membranes with enhanced stability of proton conductivity at medium temperature and high relative humidity. *Electrochimica Acta* 52 (28), 8125–8132.
- Ali, I.M., Zakaria, E.S., Ibrahim, M.M., El-Naggar, I.M., 2008. Synthesis, structure, dehydration transformations and ion exchange characteristics of iron-silicate with various Si and Fe contents as mixed oxides. *Polyhedron* 27 (1), 429–439.
- Ali, I.M., Kotp, Y.H., El-Naggar, I.M., 2010. Thermal stability, structural modifications and ion exchange properties of magnesium silicate. *Desalination* 259 (1–3), 228–234.
- Amphlett, C.B., Jones, P.J., 1964. Cation exchange on zirconium phosphate at elevated temperatures. *Journal of Inorganic and Nuclear Chemistry* 26 (10), 1759–1761.
- Devi, P.S.R., Joshi, S., Verma, R., Lali, A.M., Gantayet, L.M., 2010. Effect of gamma radiation on organic ion exchangers. *Radiation Physics and Chemistry* 79 (1), 41–45.
- El-Naggar, I.M., Zakaria, E.S., Shady, S.A., Aly, H.F., 1999. Diffusion mechanism and ion exchange equilibria of some heavy metal ions on cerium(IV) antimonate as cation exchanger. *Solid State Ionics* 122 (1–4), 65–70.
- Ferragina, C., Rocco, R.D., Giannoccaro, P., Petrilli, L., 2010. Intercalation of Ru(II) tris (1, 10-phenanthroline) complex in α - and γ -zirconium dihydrogen phosphate. Synthesis, thermal behaviour and X-ray characterization. *Materials Research Bulletin* 45 (1), 34–39.
- Guibal, E., Milot, C., Tobin, J.M., 1998. Metal-anion sorption by chitosan beads; equilibrium and kinetics studies. *Industrial and Engineering Chemistry Research* 37, 1454–1468.
- Helferich, F., 1962. *Ion Exchange*. Mc Graw Hill, New York.
- Ho, Y.S., McKay, G., 1999a. A kinetics study of dye sorption by biosorbent waste product pith. *Resources Conservation and Recycling* 25, 171–193.
- Ho, Y.S., McKay, G., 1999b. The sorption of lead(II) ions on peat. *Water Research* 33 (2), 578–584.
- Ho, Y.S., McKay, G., 1999c. Pseudo-second order model for sorption processes. *Process Biochemistry* 34 (5), 451–465.
- Inamuddin, Ismail, Y.A., 2010. Synthesis and characterization of electrically conducting poly-*o*-methoxyaniline Zr(IV) molybdate Cd(II) selective composite cation-exchanger. *Desalination* 250 (2), 523–529.
- Khan, A.A., Inamuddin, Alam, M.M., 2005. Determination and separation of Pb²⁺ from aqueous solutions using a fibrous type organic–inorganic hybrid cation-exchange material: polypyrrole thorium(IV) phosphate. *Reactive and Functional Polymers* 63 (2), 119–133.
- Khan, A.A., Inamuddin, 2006. Preparation, physico-chemical characterization, analytical applications and electrical conductivity measurement studies of an ‘organic–inorganic’ composite cation-exchanger: polyaniline Sn(IV) phosphate. *Reactive and Functional Polymers* 66 (12), 1649–1663.
- Khan, A.A., Alam, M.M., Mohammad, F., 2003. Ion-exchange kinetics and electrical conductivity studies of polyaniline Sn(IV) tungstoarsenate; (SnO₂)(WO₃)(As₂O₅)₄(–C₆H₅–NH–)₂·*n*H₂O: a new semi-crystalline ‘polymeric–inorganic’ composite cation-exchange material. *Electrochimica Acta* 48 (17), 2463–2472.

- Khan, A.M., Ganai, S.A., Nabi, S.A., 2009. Synthesis of a crystalline organic–inorganic composite exchanger, acrylamide stannic silicomolybdate: binary and quantitative separation of metal ions. *Colloids and Surfaces* 337 (1–3), 141–145.
- Lebedev, V.N., Mel'nik, N.A., Rudenko, A.V., 2003. Sorption of cesium on titanium and zirconium phosphates. *Radiochemistry* 45 (2), 149–151.
- Mardan, A., Ajaz, R., Mehmood, A., Raza, S.M., Ghaffar, Abdul, 1999. Preparation of silica potassium cobalt hexacyanoferrate composite ion exchanger and its uptake behavior for cesium⁺. *Separation and Purification Technology* 16 (2), 147–158.
- Mohan, D., Singh, K.P., 2002. Single- and multi-component adsorption of cadmium and zinc using activated carbon derived from bagasse – an agricultural waste. *Water Research* 36 (9), 2304–2318.
- Nabi, S.A., Naushad, Mu., Bushra, R., 2009. Synthesis and characterization of a new organic–inorganic Pb²⁺ selective composite cation exchanger acrylonitrile stannic(IV) tungstate and its analytical applications. *Chemical Engineering Journal* 152 (1), 80–87.
- Nabi, S.A., Shalla, A.H., 2009. Synthesis, characterization and analytical application of hybrid; acrylamide zirconium (IV) arsenate a cation exchanger, effect of dielectric constant on distribution coefficient of metal ions. *Journal of Hazardous Materials* 163 (2–3), 657–664.
- Pandit, B., Chudasama, U., 1998. A new inorgano-organic ion exchanger: chromotropic acid anchored onto zirconium molybdate. *Colloids and Surfaces* 132 (2–3), 145–151.
- Rao, C.N.R., 1993. Spectroscopic investigations of phase transitions in complex solids. *Journal of Molecular Structure* 292, 229–253.
- Rawat, J.P., Ansari, A.A., Singh, R.P., 1990. Sorption equilibria of lead(II) on some indian soils – the natural ion exchangers. *Colloids and Surfaces* 50, 207–214.
- Scheckel, K.G., Sparks, D.L., 2001. Temperature effects on nickel sorption kinetics at mineral-water interface. *Soil Science Society of America Journal* 65, 719–728.
- Shpeizer, B.G., Bakhmoutov, V.I., Zhang, P., Prosvirin, A.V., Dunbar, K.R., Thommes, M., Clearfield, A., 2010. Transition metal–alumina/silica supermicroporous composites with tunable porosity. *Colloids and Surfaces* 357 (1–3), 105–115.
- Siddiqui, W.A., Khan, S.A., Inamuddin, 2007. Synthesis, characterization and ion-exchange properties of a new and novel 'organic–inorganic' hybrid cation-exchanger: poly(methyl methacrylate) Zr(IV) phosphate. *Colloids and Surfaces* 295 (1–3), 193–199.
- Valsala, T.P., Roy, S.C., Shah, J.G., Gabriel, J., Raj, K., Venugopal, V., 2009. Removal of radioactive caesium from low level radioactive waste (LLW) streams using cobalt ferrocyanide impregnated organic anion exchanger. *Journal of Hazardous Materials* 166 (2–3), 1148–1153.
- Varshney, K.G., Rafiquee, M.Z.A., Somya, A., 2007. Effect of surfactants on the adsorption behaviour of tin(IV) phosphate, cation exchanger for alkaline earths and heavy metal ions. *Colloids and Surfaces* 301 (1–3), 224–228.
- Walker, G.M., Weatherley, L.R., 1999. Kinetics of acid dye adsorption on GAC. *Water Research* 33 (8), 1895–1899.
- Weber, W.J., Morris, J.M., 1963. Kinetics of adsorption on carbon from solutions. *Journal of the Sanitary Engineering Division – ASCE* 89, 31–39.
- Zakaria, E.S., El-Naggar, I.M., 1998. Ion-exchange selectivities of tin(IV) and iron(III) antimonates for lithium and potassium ions. *Colloids and Surfaces* 131 (1–3), 33–37.
- Zakaria, E.S., Ali, I.M., El-Naggar, I.M., 2002. Thermodynamics and ion exchange equilibria of Gd³⁺, Eu³⁺ and Ce³⁺ ions on H⁺ form of titanium(IV) antimonate. *Colloids and Surfaces* 210 (1), 33–40.